NIH Public Access
Author Manuscript
Traffic. Author manuscript; available in PMC 2009 July 26.

Published in final edited form as:
Traffic. 2007 April ; 8(4): 389–401. doi:10.1111/j.1600-0854.2007.00540.x.

Internalization and Trafficking of Cell Surface Proteoglycans and Proteoglycan-Binding Ligands

Christine K. Payne[1,2], **Sara A. Jones**[1], **Chen Chen**[1], and **Xiaowei Zhuang**[1,3,4,*]

[1]Department of Chemistry and Chemical Biology, Harvard University, 12 Oxford Street, Cambridge, MA 02138, USA

[3]Department of Physics, Harvard University, 12 Oxford Street, Cambridge, MA 02138, USA

[4]Howard Hughes Medical Institute, Harvard University, 12 Oxford Street, Cambridge, MA 02138, USA

Abstract

Using multi-color live cell imaging in combination with biochemical assays we have investigated an endocytic pathway mediated by cell surface proteoglycans, primary receptors for many cationic ligands. We have characterized this pathway for a variety of proteoglycan-binding ligands including cationic polymers, lipids, and polypeptides. Following clathrin- and caveolin-independent, but flotillin- and dynamin-dependent internalization, proteoglycan-bound ligands associate with flotillin-1-positive vesicles and are efficiently trafficked to late endosomes. The route to late endosomes differs considerably from that following clathrin-mediated endocytosis. The proteoglycan-dependent pathway to late endosomes does not require microtubule-dependent transport or PI(3)K-dependent sorting from early endosomes. The pathway taken by these ligands is identical to that taken by an antibody against heparan sulfate proteoglycans, suggesting this mechanism may be used generally by cell surface proteoglycans and proteoglycan-binding ligands without secondary receptors.

Endocytosis is an essential cellular function responsible for the uptake of nutrients and down-regulation of signaling receptors. Multiple cellular pathways exist to mediate endocytosis, among which the clathrin- and caveolin-mediated endocytic pathways are best known (1-3). However, a growing list of molecules, receptors and pathogens has been identified to enter cells through clathrin- and caveolin-independent pathways, triggering interest in the characterization of the endocytic mechanisms and trafficking itineraries of these pathways. A clathrin- and caveolin-independent pathway can exist as a constitutive internalization mechanism, such as for the interleukin 2 receptor (4) and for certain glycosyl-phosphatidylinositol (GPI)-anchored proteins (5). Clathrin- and caveolin-independent endocytosis is also used by pathogens to invade cells, either exclusively, as for the murine polyoma virus (6,7), or in combination with a conventional pathway, as is the case for the influenza virus (8,9). Even cargo that can enter through clathrin- or caveolin-mediated endocytosis may use a clathrin- and caveolin-independent pathway in the absence of clathrin or caveolin, such as for simian virus 40 (SV40) and cholera toxin B (CTB) (10,11).

In addition to determining the cargo and conditions that lead to clathrin- and caveolin-independent endocytosis, it is also desirable to understand the post-internalization trafficking itinerary following these entry mechanisms. These properties have been examined for several

*Corresponding author: Xiaowei Zhuang, zhuang@chemistry.harvard.edu
[2]Current address: School of Chemistry and Biochemistry, Georgia Institute of Technology, Atlanta, GA 30332, USA

NIH-PA Author Manuscript
NIH-PA Author Manuscript
NIH-PA Author Manuscript

NIH-PA Author Manuscript

NIH-PA Author Manuscript

NIH-PA Author Manuscript

molecular cargoes. For example, the interleukin 2 receptor is associated with detergent-resistant membrane domains and exhibits dynamin-2-dependent internalization (4). Certain GPI-anchored proteins, after internalization through clathrin-, caveolin- and dynamin-independent endocytosis, have been shown to enter Rab5-independent, GPI-anchored protein-enriched endosomal compartments (GEECs) before being trafficked to recycling endosomes (5). In the absence of caveolin, SV40 enters cells through a clathrin- and caveolin-independent mechanism, but eventually follows the same intracellular trafficking pathway as the one used by those viruses internalized through a caveolin-mediated pathway (10). Standard marker proteins for the clathrin- and caveolin-independent pathway are still lacking. The recent finding that flotillin-1 may be a marker protein associated with a clathrin- and caveolin-independent pathway(s) provides an interesting possibility for further defining these pathways (12).

In this study, we have found that cell surface proteoglycans channel a variety of ligands into a clathrin- and caveolin-independent endocytic pathway. The strong anionic charge present on the glycosaminoglycan chains of proteoglycans (13) makes them favorable binding sites for cationic polymers, lipids and polypeptides used for drug and gene delivery (14-17) as well as for pathogens, lipoproteins, growth factors and other signaling molecules (16,18). Therefore, understanding the endocytosis of cell surface proteoglycans has important implications in regulating signaling cascades as well as in delivering therapeutic materials to cells. While proteoglycan catabolism has been probed previously (19-22), certain aspects of the endocytic mechanism and trafficking itinerary of cell surface proteoglycans remain unclear.

We use a combination of multicolor live cell imaging and biochemical assays to characterize the trafficking behavior of three distinct proteoglycan-binding ligands. These ligands include a polymer, polyethylenimine (PEI); a cationic lipid mixture, Lipofectamine (LF); and a polypeptide, polyarginine (PA). PEI and LF are commonly used reagents for the delivery of DNA and small interfering RNA (siRNA) into cells (23,24). To image the delivery behavior by PEI and LF, we complexed PEI (or LF) with fluorescently-labeled DNA or siRNA to form polyplexes (or lipoplexes). PA is a ‘cell-penetrating’ peptide that can mediate the uptake of proteins and drugs into mammalian cells (25). These peptides have also been proposed as delivery vectors for diagnostic or therapeutic nanoparticles (26). To determine the pathway taken by PA to deliver nanoparticles into cells, we imaged complexes formed between PA and quantum dots (PA-QDs). The internalization and trafficking behavior of these proteoglycan-binding ligands and cell surface proteoglycans reveals a clathrin- and caveolin-independent, but flotillin- and dynamin-dependent, endocytic pathway with a trafficking itinerary that has not been observed previously.

Results

Internalization of cationic polymers, lipids and polypeptides is mediated by cell surface proteoglycans

Based on the positive charge carried by these ligands and previous work with cationic lipids, polyamines, and cell-penetrating peptides (14,27-30), we speculated that anionic proteoglycans on the cell surface may serve as binding sites for the three cationic ligands studied here. As both PEI and LF are common transfection reagents, we first tested whether transfection by these reagents depended on sulfated, anionic cell surface proteoglycans. To this end, BS-C-1 cells, a monkey kidney cell line that is both easily transfected with cationic ligands and has a flat morphology favorable for imaging, were treated with 80mMsodiumchlorate for 24 h to inhibit the activity of ATP sulfurylase, an enzyme responsible sulfation of proteoglycans in cells (31).

The sulfate groups of the proteoglycan provide the negative charge, which is the proposed domain of interaction with the cationic ligand. Immediately before transfection, the cell culture

NIH-PA Author Manuscript

NIH-PA Author Manuscript

NIH-PA Author Manuscript

medium was replaced with sodium chlorate-free medium. To prevent endocytosis due to proteoglycan regeneration, a 2 h incubation with PEI-DNA or LF-DNA was followed by dextran sulfate-induced deactivation of complexes remaining on the cell surface. The anionic charge of dextran sulfate dissociated the DNA from the PEI or LF and allowed the DNA to be removed from the cell culture, as described in Materials and Methods. Transfection efficiency was measured using b-galactosidase as a reporter gene. The expression level of b-galactosidase, determined 24 h later, showed that the sodium chlorate treatment inhibited PEI- and LF-mediated transfection in a concentration-dependent manner (Figure 1A). As an independent test of the effect of proteoglycans on transfection, experiments were also carried out with proteoglycan-deficient Chinese hamster ovary (PGD-CHO) cells. This cell line lacks xylosyltransferase, an enzyme critical for glycosaminoglycan synthesis (32,33). Compared with wild-type CHO cells, these proteoglycan-deficient cells exhibit substantially reduced transfection efficiency (Figure 1B).

Next, we tested whether the cationic ligands remained colocalized with proteoglycans during and after endocytosis. For this purpose, a fluorescent antibody against heparan sulfate [anti-heparan sulfate proteoglycan (HSPG)], the disaccharide unit present on the glycosaminoglycan chains of HSPGs, was bound to BS-C-1 cells for 10 min at 48C, a temperature at which endocytosis cannot proceed. After removing excess anti-HSPG from the medium, we incubated polyplexes with the cells at 48C for an additional 10 min and then removed excess polyplexes. Cells were then incubated at 378C to allow endocytosis for 5-30 min, and the extent of colocalization between polyplexes and anti-HSPG was determined. The colocalization level was very high (92%) throughout this period (Figure 2A,C). Experiments described below show that the internalization of polyplexes began within minutes under these conditions and nearly all polyplexes entered cells within 30 min. These results indicate that polyplexes remained colocalized with proteoglycans during and after endocytosis. For comparison, we used the same assay to determine colocalization between proteoglycans and transferrin, a ligand known to enter cells through transferrin receptors (34,35). The colocalization between transferrin and anti-HSPG over the same time period was only 20% (Figure 2B,C). Similar results were obtained using a fluorescent-labeled antibody against glypican-1, the core protein-associated GPI-linked HSPGs. Polyplexes showed 90% colocalization with anti-glypican-1, whereas transferrin only showed 23% colocalization with anti-glypican-1. These imaging results, combined with the transfection results described above, suggest that the cellular entry of polyplexes and lipoplexes is mediated by cell surface HSPGs.

To test whether PA-QDs also bind to cell surface proteoglycans, we compared the binding of PA-QDs with sodium chlorate-treated BS-C-1 cells and with normal, untreated cells. To this end, BS-C-1 cells were incubated with PAQDs at 48C for 10 min, and excess PA-QDs in the medium were removed. Cells were then immediately imaged at room temperature. Whereas untreated cells showed a large amount of bound PA-QDs, binding was strongly inhibited for sodium chlorate-treated cells (Figure 1C). As expected, cellular entry of PA-QDs was also inhibited by sodium chlorate (data not shown). Without the PA coating, the QDs did not bind to cells. These observations confirm a previous result demonstrating that PA binds to cells through cell surface proteoglycans (27). Similar binding results were obtained for polyplexes and lipoplexes (data not shown). The binding of fluorescent anti-HSPG was also inhibited by sodium chlorate treatment, indicating that the sodium chlorate treatment indeed removed the cell surface proteoglycans (Figure 1C). Control experiments with fluorescent transferrin showed that the cellular binding of transferrin was not inhibited by the sodium chlorate treatment (Figure 1C).

NIH-PA Author Manuscript

NIH-PA Author Manuscript

NIH-PA Author Manuscript

Proteoglycan-binding ligands are endocytosed by a clathrin- and caveolin-independent pathway

We took three approaches to address the potential role of clathrin- and caveolin-mediated endocytosis in the internalization of PEI, LF and PA. First, we imaged the internalization of polyplexes, lipoplexes and PA-QDs in the presence of drugs that inhibit clathrin- or caveolin-mediated endocytosis. Second, we used siRNA to knock down clathrin or caveolin and measured the effect on internalization. Third, we measured the transfection efficiency of PEI and LF in cells treated with drugs that inhibit clathrin- or caveolin-mediated endocytosis.

First, we briefly describe our criteria for determining internalization. After being added to the cell medium, polyplexes typically accumulated in endocytic vesicles within minutes. These vesicles exhibited rapid and directed movement (Figure 3A) with an instantaneous velocity characteristic of kinesin- or dynein-directed transport on microtubules (36). A similar transport mechanism for PEI has been recently reported (37). These movements were inhibited by nocodazole, a microtubule-disrupting drug (Figure 3A), and are distinct from motion on the cell surface. Dextran sulfate, which carries a strong anionic charge, can be used to dissociate the fluorescently-labeled siRNA from the PEI after polyplex formation. Washing the cells with 50 mg/mL dextran sulfate thus removed the fluorescent signal from polyplexes on the plasma membrane. However, the addition of dextran sulfate to the cell medium did not result in the loss of fluorescent signal from polyplexes undergoing rapid, directed motion (data not shown). These features indicated that the polyplex-containing vesicles were transported on microtubules inside cells. We used this microtubule-dependent movement as a signal to indicate that polyplexes have already been internalized into intracellular vesicles. By these criteria, nearly 100% of the polyplexes entered BS-C-1 cells within 30 min. The use of rapid motion as an indication of entry may lead to an error in measurement caused by endosomes that remain stationary during the entire period of observation. As discussed in Materials and Methods, we estimate this error to be less than 10% for all ligands studied here.

To inhibit clathrin-mediated endocytosis, BS-C-1 cells were treated with 5 mg/mL chlorpromazine for 30 min prior to the addition of the polyplexes. This treatment completely blocked the endocytosis of human low-density lipoprotein (LDL) (Figure 3B), a ligand known to enter cells through clathrin-mediated endocytosis. In comparison, chlorpromazine did not inhibit the entry of polyplexes (Figure 3B). Filipin and nystatin, cholesterol-binding drugs that inhibit caveolin-mediated endocytosis, also did not inhibit polyplex entry (Figure 3B, nystatin not shown). In comparison, the entry of CTB, which is known to enter cells through caveolae (38,39), was inhibited by filipin (Figure 3B). While CTB can use other endocytic pathways (11,12), the results shown here, together with our previous observation that CTB shows nearly 100% colocalization with caveolin-1 in BS-C-1 cells (9), indicate that the internalization of CTB in these cells is caveolin-dependent. Similar results with chlorpromazine and filipin were also observed for lipoplexes, PA-QDs and anti-HSPG (Figure 3B). While chlorpromazine treatment did not block the entry of CTB and filipin treatment did not block the entry of LDL (Figure 3B), it is worth noting that the inhibitory effects of these drugs may not be entirely specific. For example, chlorpromazine may inhibit some clathrin-independent endocytic pathways. However, the ability of chlorpromazine to inhibit clathrin-mediated endocytosis, as shown by the LDL control, taken together with our observation that chlorpromazine did not inhibit the internalization of these proteoglycan-binding ligands, strongly suggests that their entry was not mediated by clathrin. Similarly, the observation that filipin and nystatin did not inhibit internalization provides strong evidence that the entry of these ligands was also caveolin-independent.

To more specifically inhibit clathrin- or caveolin-mediated endocytosis, we used siRNA to knock down the expression level of clathrin and caveolin in cells. As the clathrin sequence is available for the human genome but not for monkey, we tested clathrin and caveolin

NIH-PA Author Manuscript

NIH-PA Author Manuscript

NIH-PA Author Manuscript

knockdown in human (HeLa) cells. Non-targeting (non-specific) siRNA transfected cells were used as controls. The knockdown efficiency was tested by immunofluorescence as well as by the endocytosis of transferrin, which enters cells through clathrin-mediated endocytosis, and of CTB, which enters cells through caveolin-mediated endocytosis (Figure 3C,D). A cotransfected enhanced yellow fluorescent protein (EYFP) marker was used to locate knockdown cells. Using immunofluorescence, we determined that 76% of cells exhibited substantial clathrin knockdown and 68% of cells exhibited substantial caveolin knockdown, i.e. these cells did not show detectable immunofluorescence for clathrin or caveolin, respectively. Notably, whereas only a fraction of clathrin- or caveolin knockdown cells expressed the cotransfected EYFP marker, all cells expressing EYFP exhibited clathrin or caveolin knockdown. The EYFP-expressing cells were used for ligand uptake analysis. Cells were incubated with each ligand for 30 min. The efficiency of entry was determined using the assay described above for the drug studies. As expected, the entry efficiency of transferrin in clathrin knockdown cells was very low, only 2% when compared with amount of transferrin that entered control cells treated with nonspecific siRNA (Figure 3D). CTB showed only 7% entry into caveolin knockdown cells, again normalized against the amount of CTB entry in control cells transfected with non-specific siRNA (Figure 3D). In comparison with these clathrin- and caveolin-dependent ligands, polyplexes and anti-HSPG were not significantly inhibited by siRNA against clathrin or caveolin (Figure 3D). Polyplexes showed 95% internalization efficiency for clathrin knockdown cells and 70% internalization efficiency for caveolin knockdown cells, normalized against the amount of entry observed for control cells. Anti-HSPG showed 87% entry efficiency for clathrin knockdown cells and 103% for caveolin knockdown cells, normalized against results from control cells.

To further test whether the clathrin- and caveolin-independent pathway exploited by these ligands is related to their gene delivery activity, we examined PEI- and LF-mediated transfection by measuring the expression level of a delivered b-galactosidase gene, as shown in Figure 1A,B. In BS-C-1 cells treated with 5mg/mL chlorpromazine, a concentration sufficient to block clathrin-mediated endocytosis of LDL, the PEI- and LF-mediated transfection efficiencies were 90 and 95%, respectively, compared with untreated cells. In cells treated with 5 mg/mL filipin, a concentration sufficient to block caveolin-mediated endocytosis of CTB, the PEI- and LF-mediated transfection efficiencies were 135 and 70%, respectively. The error in the transfection measurements was determined to be 10% based on results from three independent experiments. Taken together, these results strongly suggest that the polyplexes, lipoplexes and PA-QDs enter cells through a clathrin- and caveolin-independent pathway.

Internalization of proteoglycan-binding ligand is dynamin-dependent

Two approaches were used to test the role of dynamin in the internalization of the proteoglycan-binding ligands using the polyplexes as a representative ligand. First, BS-C-1 cells were treated with Dynasore, a cell permeable drug that inhibits dynamin-1 and dynamin-2 (40). Dynasore treatment successfully blocked the internalization of transferring (Figure 4A), which is known to require dynamin for internalization (41). Notably, Dynasore also inhibited the internalization of the polyplexes. The polyplex uptake was only 15%comparedwith untreated control cells (Figure 4A).

As an alternative method to investigate the dynamin dependence for internalization, we used siRNA to knock down the expression level of dynamin-2 in HeLa cells. The knockdown efficiency was tested by immunofluorescence as well as by the endocytosis of transferrin (Figure 4B). Again, a cotransfected EYFP marker was used to mark knockdown cells. Using immunofluorescence, we determined that 58% of cells exhibited substantial dynamin-2 knockdown. Whereas not all these dynamin-2 knockdown cells expressed the EYFP marker,

NIH-PA Author Manuscript

NIH-PA Author Manuscript

NIH-PA Author Manuscript

all cells expressing EYFP exhibited dynamin knockdown. The EYFP-expressing cells were used for ligand uptake analysis. Cells were incubated with polyplexes for 30 min and the efficiency of entry was determined using the assay described above. While the amount of transferrin that entered control cells treated with non-specific siRNA was high, the entry efficiency of transferrin in dynamin-2 knockdown cells was not detectable. Similar to transferrin, polyplexes showed only 2% internalization efficiency for dynamin-2 knockdown cells compared with control cells treated with non-specific siRNA (Figure 4B).

Proteoglycan-binding ligands colocalized with flotillin-1

Recent reports have shown that flotillin-1 serves as amarker for a clathrin- and caveolin-independent pathway (12). To test the possible involvement of flotillin-1 with the clathrin and caveolin-independent pathway used by the cationic ligands, we measured the colocalization of enhanced green fluorescent protein (EGFP)-flotillin-1with the cationic ligands and anti-HSPG. PEI, lipoplexes, PA-QDs and anti-HSPG all showed substantial colocalization with EGFP-flotillin-1 within the first 10 min following binding (Figure 5A,C). Specifically, PEI showed 91% colocalization, lipoplexes 84%, PA-QDs 78% and anti-HSPG 82%. In comparison, transferrin and LDL, both classical markers of the clathrin-mediated pathway showed only 9% colocalization with EGFP-flotillin-1 within the same time period (Figure 5B,C).

To test whether flotilin-1 is required for the uptake of proteoglycan-binding ligands, we also used siRNA against flotillin-1. Seventy-two percent of cells showed flotillin-1 knockdown as measured by immunofluorescence. To mark knockdown cells, we again used a cotransfected EYFP marker as described above for clathrin, caveolin and dynamin-2 knockdown. Non-specific siRNA was used as a control. Cells were incubated with polyplexes for 30 min. The efficiency of entry was determined using the assay described above. siRNA against flotillin-1 inhibited the internalization of the polyplexes with a 69% decrease in internalization compared with control cells, whereas transferrin entry, used as a control, was not significantly inhibited by flotillin knockdown (Figure 5D).

Proteoglycan-binding ligands are efficiently trafficked to late endosomes

To further determine the intracellular trafficking pathway of these proteoglycan-binding ligands, we imaged the ligands simultaneously with early and late endosomes that were marked by fluorescent proteins fused to specific Rab guanosine triphosphatases (42-47). Rab5 has been used previously as an early endosomal marker (42,43) and Rab7 and Rab9 have been used as late endosomal markers (42,44). To confirm that these fluorescent Rab proteins indeed label the intended endosomes, we first imaged them together with independent endosomal markers. As expected, Rab5 showed a high degree of colocalization (80%) with early endosomal antigen 1 (EEA1) (Figure 6A). It was previously established that LDL is trafficked to late endosomes and lysosomes for degradation and accumulates in late endosomes within 1 h following endocytosis (48,49). Indeed, 89%of LDL particles colocalized with Rab9- positive endosomes at 1 h after endocytosis (Figure 6B). In cells expressing both enhanced cyan fluorescent protein (ECFP)-Rab7 and EYFP-Rab9, discrete Rab9 structures and Rab7 structures showed a high degree of colocalization (91%; data not shown), consistent with previous findings (44). We have also shown that PEI- and LF-mediated transfection was not inhibited by the expression of fluorescent Rab proteins and that the trafficking of LDL was unperturbed (data not shown), consistent with previous findings that the low expression level used for these fluorescent-labeled Rab proteins does not compromise the function of the endosomes (43-47).

We imaged polyplexes simultaneously with EYFP-Rab5 or EYFP-Rab9 at various times after endocytosis to monitor the trafficking behavior of PEI. The following criteria were used to judge colocalization with a specific endosome: ligands were considered to be colocalized with

NIH-PA Author Manuscript

NIH-PA Author Manuscript

NIH-PA Author Manuscript

an endosome only if they showed significant spatial overlap and moved together for a minimum of 20 seconds. By observing the motion of the endosome and ligand, rather than a static image,we ensured that we were measuring true colocalization rather than a noninteracting, chance overlap within the same detection volume. By these criteria, the fraction of polyplexes colocalized with Rab5-labeled early endosomes remained low after endocytosis and decayed to an undetectable level within 60 min (Figure 6C,E). The extent and time-dependence of colocalization with EEA1 mirrored the results for Rab5 (data not shown), consistent with the high colocalization obtained between Rab5 and EEA1. Colocalization with Rab9-labeled late endosomes increased steadily to nearly 100%within 2 h (Figure 6D,E). Similar trends in colocalization with Rab5 and Rab9 were observed for lipoplexes, PA-QDs and anti-HSPG (data not shown). While the Golgi has also been found to contain Rab9 (44), we did not observe the accumulation of these ligands in the Golgi region. In addition, the colocalization between these ligands and Rab7, another late endosomal marker, was nearly identical to that observed with Rab9 (data not shown). These results indicate that all three proteoglycan-binding ligands and anti-HSPG were efficiently trafficked to late endosomes, consistent with a previous result showing that a cell-penetrating peptide colocalizes extensively with acidic endocytic compartments (29). As a control, we tested the time-dependent colocalization of LDL with Rab5 and Rab9 (Figure 6F). As expected for LDL, we observed high colocalization of LDL with Rab5 at early time-points, which peaked at about 80%, followed by a steady decrease in colocalization to 20% at 1 h. In comparison, LDL colocalization with Rab9 increased steadily to 90% at 30 min and remained greater than 90% until at least 1 h after endocytosis. It has been shown previously that a fraction of endosomes contain both early and late endosome markers (45-47), potentially representing an intermediate phase of endosome maturation. A significant fraction of LDL is delivered to these intermediate endosomes (47). Thus, the fractions of LDL colocalizing with Rab5 and Rab9 added up to more than 100%at certain time-points.

Microtubules are not required for trafficking to late endosomes

Conventional transport from early to late endosomes requires microtubules (50). We sought to address whether microtubule transport was required for proteoglycan-binding ligands to enter late endosomes. We incubated BS-C-1 cells with nocodazole to disrupt microtubules. As expected, the rapid and directed movement of the endocytic vesicles containing proteoglycan-bound ligands was inhibited (Figure 3A). However, the colocalization of polyplexes with Rab5 or Rab9 endosomes was only slightly affected. The maximum percentage of polyplexes colocalized with Rab5 endosomes remained similar to that in untreated cells, but the decay rate from the maximum was slower (Figure 6E). The rate of entry into late endosomes is largely unaffected, but the final colocalization (measured at 2 h after endocytosis) was reduced by 20%, consistent with the increased colocalization with early endosomes at the same time (Figure 6E). Similar results were obtained for lipoplexes, PA-QDs and anti-HSPG (Figure 7A). The trafficking of LDL to late endosomes was, however, substantially inhibited in nocodazole-treated cells. Unlike in untreated cells, where most of the LDL particles were trafficked to late endosomes containing Rab9, but not Rab5, in nocodazole-treated cells, the majority of LDL showed an overlap with both Rab5 and Rab9 at 1 h after endocytosis (Figure 7A). This result indicates that in microtubule- disrupted cells, LDL was trapped in endosomal maturation intermediates that contained both early (Rab5) and late (Rab9) endosome markers (45-47), whereas the proteoglycan-binding ligands are still efficiently trafficked to late endosomes.

Phosphatidylinositol 3-phosphate-mediated sorting is not required for entry into late endosomes

Both early endosome fusion and the sorting of certain cargo from early to late endosomes require the activity of phosphatidyl-inositol-3-OH kinase [PI(3)K] (51-54). The activity of PI (3)K can be specifically disrupted using the fungal toxin wortmannin (51,55,56). By disrupting PI(3)K activity, we can test the role of early endosomal sorting in the intracellular transport of

NIH-PA Author Manuscript

NIH-PA Author Manuscript

NIH-PA Author Manuscript

cationic ligands. The transport of LDL from early to late endosomes was severely inhibited by the 30 min pretreatment of cells with 240 nM wortmannin. In untreated cells, the majority of LDL colocalized with Rab9 at 1 h after endocytosis (Figure 7B). Wortmannin treatment resulted in a nearly four-fold decrease in the colocalization of LDL with Rab 9 and a substantial retention of LDL in the Rab5 marked endosomes at the same time-point (Figure 7B), suggesting LDL was no longer sorted efficiently from the early endosomes to the late endosomes. In contrast, the transport of polyplexes, lipoplexes, PA-QDs and anti-HSPG to late endosomes was essentially uninhibited by wortmannin (Figure 7B). While wortmannin has been shown to prevent many types of cargo, including Semliki Forest virus (55), EGF receptor (53) and LDL, as shown here, from reaching late endosomes, results for bulk fluids have been mixed. For example, trafficking of horseradish peroxidase to a degradative pathway was blocked by wortmannin, but trafficking of Lucifer yellow (56) and dextran (53) was not blocked. As such, while our results suggest the interesting possibility that the proteoglycan-binding ligands can be trafficked to late endosomes directly, without sorting from early endosomes, it remains possible that these ligands are delivered from early to late endosomes by a non-specific mechanism similar to the behavior of some bulk fluids.

Discussion

A substantial range of endocytic cargo, including signaling receptors, nutrients, toxins and viruses, enters cells independently of both clathrin and caveolin. While likely encompassing numerous endocytic pathways, they have been grouped in the category of ‘clathrin- and caveolin-independent endocytosis. We have shown that three distinct proteoglycan-binding ligands, PEI, LF and PA, entered cells by a clathrin- and caveolin-independent, but dynamin- and flotillin-dependent, mechanism (Figures 3-5). The post-endocytic trafficking observed for this pathway showed important differences compared with the clathrin and caveolin-mediated pathways. Cargo trafficked along this pathway colocalized with flotillin-1-positive vesicles (Figure 5). After internalization, cargo was delivered into late endosomes with high efficiency (Figure 6). The majority of cationic ligands were delivered to late endosomes without requiring microtubule-dependent transport or phosphatidylinositol 3-phosphate (PtdIns3P)-dependent sorting from early endosomes to multi-vesicular bodies, possibly bypassing the early endosomes (Figure 7). In contrast, PtdIns3P-dependent sorting from the early endosome and microtubule-dependent trafficking to the late endosome are two hallmarks of the postendocytic trafficking pathway following clathrin-dependent endocytosis (50,54,57).

The above results indicate that the three proteoglycan-binding ligands, PEI, LF and PA, have similar internalization and trafficking mechanisms. No secondary endocytic receptor has been identified for these ligands nor are they likely to have the same secondary receptor, considering their distinct chemical structures. It is therefore possible that their endocytic trafficking is directed by their common primary receptor, cell surface proteoglycans. This model is supported by our observation that the internalization mechanism and post-endocytic trafficking behavior of cell surface proteoglycans, reported by an antibody against HSPG (anti-HSPG), were highly similar to those observed for the three proteoglycan-binding ligands (Figures 3, 5 and 7). Moreover, immediately following entry, polyplexes are nearly 100% colocalized with anti-HSPG within the same vesicles (Figure 2).

The proteoglycan-dependent trafficking pathway described above is distinct from previously identified clathrin- and caveolin-independent pathways. For example, interleukin 2 receptors are associated with detergent-resistant membrane domains, internalized in a dynamin-dependent manner and delivered to early endosomes (4). GPI-anchored proteins are internalized independently of dynamin and trafficked through specific early endosomal compartments, GEECs, devoid of conventional early endosome markers such as Rab5, before reaching recycling endosomes (5). Some GPI-anchored proteins have also been shown to

NIH-PA Author Manuscript

NIH-PA Author Manuscript

NIH-PA Author Manuscript

colocalize with flotillin-1 (12) and possibly the Golgi apparatus (58). SV40 takes a caveolar-like pathway in route to the endoplasmic reticulum (ER) (10). The antimicrobial peptide LL-37 likely enters cells through a caveolin-independent, but lipid raft-dependent, pathway (30). In comparison, the entry of the cationic, proteoglycan-binding ligands studied in this work did not appear to involve cholesterol-enriched membrane domains, as indicated by the lack of effect of filipin and nystatin on the internalization of these ligands. The internalization of these ligands was dynamin-dependent. The proteoglycan-binding ligands showed high colocalization with flotillin-1, and the destination of these ligands appeared to be late endosomes instead of Golgi, recycling endosomes or the ER. At early times, the trafficking path of these ligands may intersect with the routes taken by other clathrin- and caveolin-independent cargo, for example at flotillin-positive vesicles or GEECs. A full characterization of the early endocytic compartments for these proteoglycan-dependent ligands remains to be elucidated. It was previously reported that the flotillin-dependent entry pathway of CTB and GPI-anchored proteins is dynamin-independent (5,12). Here, we show that entry of the proteoglycan-binding ligands requires both flotillin and dynamin. This difference suggests that flotillin-1 may play a role in multiple endocytic pathways, both dynamin-dependent and independent.

As the cationic ligands described here are commonly used for gene delivery, it is interesting to consider how the observed endocytic pathway may relate to the ability of these ligands to productively deliver genes into the cell. Unfortunately, release of the complexes from late endosomes was observed to be a rate-limiting step and occurred rarely, such that we were unable to track entry of DNA or siRNA into the cytoplasm and ultimately into the nucleus. While our direct imaging experiments use lower concentrations of cationic ligands than that recommended for transfection, we found that increasing the concentration to the normal transfection concentration did not lead to visible endosomal release of the complexes. Our transfection experiments, using high concentrations of cationic ligands, demonstrated that transfection by PEI and LF required proteoglycans, but not clathrin or caveolin. Therefore, it is likely that productive transfection by PEI and LF uses the entry and trafficking pathway described in this study. In the event that this pathway does not lead to productive gene delivery, it remains an important consideration for the rational design of cationic vectors as the majority of polyplexes, lipoplexes and PA-QDs entered cells through this pathway.

In summary, we have identified a constitutive clathrin- and caveolin-independent endocytic pathway used by HSPGs, primary receptors for many ligands essential for cell maintenance and signaling (16,18). Cationic ligands with important applications in gene, protein and drug delivery, such as cationic polymers, lipids and polypeptides, are internalized, along with cell surface proteoglycans, through this pathway. By tracking the interaction of these proteoglycan-binding ligands with endocytic structures in real time, we have found that this entry pathway leads to an intracellular trafficking itinerary that is distinct from previously described endocytic pathways. These cationic ligands entered cells with a dynamin-dependent mechanism, associated with flotillin-1-positive vesicles, and ultimately accumulated in late endosomes. The majority of the proteoglycanbinding ligands were delivered to late endosomes without requiring intact microtubules or PtdIns3P-dependent sorting through early endosomes, possibly bypassing conventional early endosomes. The endocytic pathway described here reflects an intrinsic endocytic pathway for the downregulation of HSPGs at the cell surface and is therefore likely to be a general pathway used by other proteoglycan-binding ligands that lack secondary endocytic receptors.

NIH-PA Author Manuscript

NIH-PA Author Manuscript

NIH-PA Author Manuscript

Materials and Methods

Cell culture

BS-C-1 and HeLa S3 (ATCC, Manassas, VA) cells were maintained in a 37°C, 5% carbon dioxide environment in Dulbecco's modified Eagle's medium (DMEM, Invitrogen, Carlsbad, CA) with 10% (v/v) fetal bovine serum (FBS, Invitrogen). Wild-type and mutant (pgsA-745) CHO (ATCC) cells were maintained in a 37°C, 5% carbon dioxide environment in F-12K medium (ATCC) with 10% (v/v) FBS.

Wild type and mutant CHO cells were only used for the experiments described in Figure 1B. HeLa cells were only used for the siRNA knockdown experiments described in Figure 3C, 3D, 4B and 5D. All other experiments used BS-C-1 cells. Cells were passaged every 3 days. For fluorescence imaging, cells were cultured in 60 mm glass-bottom cell culture dishes (MatTek, Ashland, MA).

Fluorescent labeling of cationic ligands: Polyplexes, lipoplexes, PA-QDs, anti-HSPG, and additional endocytic ligands

PEI (*in vitro* jetPEI, Qbiogene, Morgan Irvine, CA) and LF (Invitrogen) were complexed with 22 base pair Cy5- or TMR-labeled siRNA (Dharmacon, Lafayette, CO) to form polyplexes and lipoplexes, respectively, according to the manufacturers' instructions. Directly labeling PEI with Cy5 (Amersham/GE Healthcare, Piscataway, NJ) or complexing PEI with TOTO (Invitrogen)-labeled DNA results in the same intracellular pathway (data not shown). PEI-DNA (or PEI-siRNA) was formed with an N to P ratio of 8 as we found this ratio to be optimal for transfection of the BS-C-1 cells. PA was conjugated with fluorescent quantum dots (PA-QDs). To form PA-QDs, streptavidin-labeled quantum dots with an emission of 705 nm (Quantum Dot Corporation) were incubated with biotinylated polyarginine according to the manufacturer's instructions. In the absence of polyarginine, no cellular binding or entry of quantum dots was observed. Antibodies against proteoglycans (MAB2040, Chemicon, Temecula, CA; referred to as anti-HSPG and GPC1, Abnova, Taipei City, Taiwan; referred to as anti-glypican-1) were labeled with Cy5 (Amersham) according to the manufacturer's instructions.

In addition to the cationic ligands, a number of well-characterized ligands were used for control experiments. Transferrin, labeled with TMR or Alexa647, and Cholera toxin B (CTB), labeled with Alexa647, were purchased from Invitrogen. LDL (MP Biomedical) was labeled with DiD (Invitrogen) at a concentration of 0.5 μM and mixed gently for 1 hour before removal of excess dye on a Nap5 column (Amersham).

Expression of fluorescently-labeled endocytic proteins

For imaging flotillin-1, early endosomes, or late endosomes, BS-C-1 cells were transfected with flotillin-1-EGFP (a gift from B. J. Nichols), EYFP-Rab5 (a gift from M. Zerial), ECFP-Rab7, or EYFP-Rab9 (gifts from S. Pfeffer). Transfections were performed with the FuGENE 6 (Roche, Indianapolis, IN) transfection reagent 24 hours after plating. Experiments were carried out approximately 48 hours following transfection with the exception of flotillin-1-GFP, which was imaged 24 hours after transfection.

Drug treatments

To remove cell surface proteoglycans, cells were incubated with sodium chlorate ($NaClO_3$) at the specified concentration for 24 hours prior to transfection experiments and 48 hours prior to binding experiments. No difference was observed between the 24 and 48 hour pretreatment, the longer pretreatment was used to grow cells to the appropriate confluency for imaging. Chlorpromazine (5 μg/mL), filipin (5 μg/mL) or nystatin (25 μg/mL) was used to inhibit

NIH-PA Author Manuscript

NIH-PA Author Manuscript

NIH-PA Author Manuscript

clathrin- or caveolin-medaited endocytosis. Wortmannin (240 nM) was used to inhibit PI(3) K. Nocodazole (60 μM, Calbiochem, San Diego, CA) was used to disrupt microtubules. Dynasore (80 μm, synthesized by H. Pelish and a gift from T. Kirchhausen) was incubated with the cells in serum-free PBS-glucose. All drugs, with the exception of sodium chlorate, were added to cells 30 minutes prior to experiments and remained present during the experiments. The efficiency of each drug treatment was tested with control ligands as described in the text. Dextran sulfate, 50 μg/mL, was used, as described in the text, to remove the DNA or siRNA associated with polyplexes that had not been internalized and remained bound to the plasma membrane. The effect of dextran sulfate was to cause the dissociation of siRNA from PEI. This was tested using Cy5-labeled PEI and TMR-labeled siRNA cold bound to the cell. After dextran sulfate treatment, the siRNA signal was removed from the cell surface while the PEI remained bound and was able to enter the cells upon warming. All reagents were from Sigma-Aldrich (St. Louis, MO) unless otherwise noted.

siRNA knockdown

Approximately 10^5 HeLa S3 (ATCC) cells were seeded in each well of a 6-well plate 24 hours before transfection. For transfection, 10 μL of OligofectAMINE (Invitrogen) were added to 20 μL Opti-MEM I (Invitrogen) and the solution was incubated for 5-10 minutes at room temperature. This mixture was then added to a second solution of 5 μL of siRNA (40 μM) and 158 μL Opti-MEM I and allowed to complex for 15-20 minutes at room temperature. After incubation, 807 μL of Opti-MEM I were added to the OligofectAMINE/siRNA solution and the resulting 1 mL was added to the cells. Four hours after the addition of the solution, 4 mL of DMEM with 20% FBS was added. On day 2, cells were trypsinized and seeded into 6 cm plates. On day 3, cells were transfected with siRNA again according to the above procedure, only scaled by a factor of 1.5 to compensate for the larger dish area. In this second round of transfection with siRNA, cells were cotransfected with an EYFP plasmid for use as a marker using the FuGENE 6 (Roche), transfection procedure described above. On day 4 cells were trypsinized again and split into glass-bottomed culture dishes for experiments. A scrambled, non-specific siRNA construct was used as a control (siCONTROL Non-targeting siRNA 1, Dharmacon). siRNA against clathrin heavy chain was described previously (55), siRNA against human caveolin-1 was obtained from Qiagen (HS_CAV1_10_HP), siRNA against dynamin-2 was obtained from Qiagen (HS_DNM2_8_HP), and siRNA against flotillin-1 was a combination of UGAGGCCAUGGUGGUCUCCdTdT from Dharmacon and Santa Cruz Biotechnology (Santa Cruz, CA, Catalog Number: 35391) (12).

Cellular binding assay

Cells were cooled to 4°C for 5 minutes before the addition of polyplexes (50 μL, 20% of recommended transfection amount), lipoplexes (50 μL, 5% of recommended transfection amount), PA-QDs (10 μL, 2% of recommended cell labeling amount), heparan sulfate antibodies (40 μL, 1:500 dilution of labeled antibody), transferrin (10 μg/mL), or cholera toxin B (100 μg/mL). Lower concentrations of polyplexes were used for imaging to avoid extensive fluorescence background. Ligands were allowed to bind for 10 minutes at 4°C at which point cells were rinsed twice with chilled MEM and then imaged with the excitation laser intensity held constant. Sodium chlorate was removed from the medium before the addition of the ligands.

Cellular entry assay

Ligands, at the same concentration as for the cell binding assay, were added to cells at 37°C and incubated for the time noted in the text. Additionally, DiD labeled LDL was used at a concentration of 33 μg/mL. The amount of polyplexes, lipoplexes, or anti-HSPG that entered cells was determined by measuring the total fluorescent signal included within endocytic

NIH-PA Author Manuscript

NIH-PA Author Manuscript

NIH-PA Author Manuscript

compartments that show microtubule-dependent movement. This method may result in an underestimate as stationary endosomes would not be included. Based on the number of stationary spots, this underestimate, at maximum, gives 5%, 7%, and 5% error for polyplexes, lipoplexes, and HSPG antibody, respectively. Aggregates greater than 1 μm in size, distinguished with light microscopy, were not counted. PA-QD entry was measured by counting the number of PA-QDs undergoing microtubule-dependent movement as compared to diffusive movement on the cell surface. Typically 10% of the PA-QD particles were stationary and were not included in the measurement. The amount of tranferrin and CTB that entered cells was determined by comparing the fluorescent signal of tranferrin (or CTB) in drug- or siRNA-treated cells with results obtained in control cells after an acid wash (0.2 M acetic acid, 0.2 M NaCl in PBS, rinsed twice at 4°C) was used to remove transferrin and CTB bound to cell surface. For the measurements of heparan sulfate antibodies with polyplexes or transferrin, cells were chilled to 4°C and anti-HSPG was cold bound to the cells for 10 minutes. The cells were then rinsed twice with DMEM with 10% FBS prior to the addition of the polyplexes (or transferrin) which were then cold bound for an additional 10 minutes. Cells were washed twice with MEM and incubated at 37°C for the specified time.

Transfection assay

Transfection efficiency was measured 24 hours post-transfection by a -galactosidase assay (Promega, Madison, WI), according to the manufacturer's instructions. PEI or LF was complexed with a - galactosidase plasmid. The expression of this plasmid was measured by adding o-nitrophyl-B-D-galactopyranoside (ONPG) to lysed cells. The conversion of ONPG to the yellow o-nitrophenol by□ - galactosidase was measured with a UV-Vis spectrophotometer. To determine the transfection efficiency in the presence of drugs, cells were pretreated with the drug for 30 minutes and incubated with full concentrations of PEI-DNA or LF-DNA complexes for two hours in the presence of the drug. The cells were then treated with 50 μg/mL dextran sulfate to deactivate any complex that had not been internalized and the drug was then removed to reduce possible adverse effects on cells. Dextran sulfate causes the dissociation of DNA from PEI, but not PEI from cells. The addition of dextran sulfate simultaneously with the transfection reagent results in no transfection (data not shown). Transfection efficiency was normalized against control experiments carried out with untreated cells.

Immunofluorescence

Immunofluorescence was based on standard protocols. Cells were fixed with 2% formaldehyde at 40 minutes at room temperature and then permeabilized (3% BSA, 10% FBS, 0.5% Triton-X100 in PBS) for 15 minutes at room temperature. The primary antibody (1 mg/mL) was added to the cells at a 1:200 dilution and incubated overnight at 4°C. The secondary antibody (1 mg/mL) was added to the cells (in 0.2% BSA and 0.1% Triton-100 in PBS) at a 1:1000 dilution and incubated at room temperature for 30 minutes. Cells were washed three times with 0.2% BSA and 0.1% Triton-100 in PBS between each step. Anti-EEA1 and anti-Flotillin-1 monoclonal antibodies were obtained from BD Biosciences (San Jose, CA). Anti-Clathrin Heavy Chain and Anti-Caveolin-1 antibodies were from Santa Cruz Biotechnologies. All secondary antibodies were purchased from Invitrogen.

Fluorescence imaging

Cy5, Alexa647, and DiD were excited with a 633 nm helium-neon laser (Melles-Griot, Carlsbad, CA). Quantum dots, EYFP, and TMR were excited with a 532 nm diode laser (Crystalaser, Reno, NV). EGFP was excited with the 488 nm line and ECFP with the 457 nm line of an argon ion laser (Melles Griot). An inverted microscope (Olympus IX70, Center Valley, PA) in an epi-fluorescent configuration with an oil-immersion objective (N.A. = 1.45,

NIH-PA Author Manuscript

NIH-PA Author Manuscript

NIH-PA Author Manuscript

60x, Olympus) was used for imaging. Long and short wavelength emissions were spectrally separated by a 650 nm long-pass dichroic mirrors (Chroma, Rockingham, VT), and imaged onto a CCD camera (Roper Scientific, Tucson, AZ, CoolSnap HQ). A 665 nm longpass filter was used for Cy5 or QD detection, a 585/35 nm bandpass filter was used for EYFP and TMR, a 535/20 nm bandpass filter for EGFP, and a 480/40 nm bandpass filter for ECFP. Images were typically recorded at a rate of 1 frame/second with a 500 ms exposure. Image analysis has been described previously (9).

Immediately before imaging experiments, cells were washed with phenol red-free minimum essential medium with 1% glucose. Glucose oxidase (0.2 mg/mL) with catalase (1 μL/mL) was used as an oxygen scavenger. Unless otherwise noted, experiments were conducted at 37°C.

Acknowledgments

We thank M. Zerial, S. Pfeffer, and B. Nichols for their generous gifts of the ECFP-Rab5, ECFP-Rab7, EYFP-Rab9, and GFP-flotillin-1 plasmids. We thank Tomas Kirchhausen and Henry E. Pelish for the gift of Dynasore. This work is supported in part by the National Institute of Health (NIGMS), the Howard Hughes Medical Institute, the Kinship Foundation, the Arnold and Mabel Beckman foundation (to X.Z.), and a National Science Foundation center grant (to the NSEC, Harvard). C.K.P. is partially supported by a Ruth L. Kirschstein National Research Service Award from the National Institutes of Health.

References

1. Nichols BJ, Lippincott-Schwartz J. Endocytosis without clathrin coats. Trends Cell Biol 2001;11:406–412. [PubMed: 11567873]
2. Conner SD, Schmid SL. Regulated portals of entry into the cell. Nature 2003;422:37–44. [PubMed: 12621426]
3. Pelkmans L, Helenius A. Insider information: what viruses tell us about endocytosis. Curr Opin Cell Biol 2003;15:414–422. [PubMed: 12892781]
4. Lamaze C, Dujeancourt A, Baba T, Lo CG, Benmerah A, Dautry-Varsat A. Interleukin 2 receptors and detergent-resistant membrane domains define a clathrin-independent endocytic pathway. Mol Cell 2001;7:661–671. [PubMed: 11463390]
5. Sabharanjak S, Sharma P, Parton RG, Mayor S. GPI-anchored proteins are delivered to recycling endosomes via a distinct cdc42-regulated, clathrin-independent pinocytic pathway. Dev Cell 2002;2:411–423. [PubMed: 11970892]
6. Gilbert JM, Benjamin TL. Early steps of polyomavirus entry into cells. J Virol 2000;74:8582–8588. [PubMed: 10954560]
7. Ewers H, Smith AE, Sbalzarini IF, Lilie H, Koumoutsakos P, Helenius A. Single-particle tracking of murine polyoma virus-like particles on live cells and artificial membranes. Proc Natl Acad Sci U S A 2005;102:15110–15115. [PubMed: 16219700]
8. Sieczkarski SB, Whittaker GR. Influenza virus can enter and infect cells in the absence of clathrin-mediated endocytosis. J Virol 2002;76:10455–10464. [PubMed: 12239322]
9. Rust MJ, Lakadamyali M, Zhang F, Zhuang X. Assembly of endocytic machinery around individual influenza viruses during viral entry. Nat Struct Mol Biol 2004;11:567–573. [PubMed: 15122347]
10. Damm EM, Pelkmans L, Kartenbeck J, Mezzacasa A, Kurzchalia T, Helenius A. Clathrin- and caveolin-1-independent endocytosis: entry of simian virus 40 into cells devoid of caveolae. J Cell Biol 2005;168:477–488. [PubMed: 15668298]
11. Kirkham M, Fujita A, Chadda R, Nixon SJ, Kurzchalia TV, Sharma DK, Pagano RE, Hancock JF, Mayor S, Parton RG. Ultrastructural identification of uncoated caveolin-independent early endocytic vehicles. J Cell Biol 2005;168:465–476. [PubMed: 15668297]
12. Glebov OO, Bright NA, Nichols BJ. Flotillin-1 defines a clathrin-independent endocytic pathway inmammalian cells. Nat Cell Biol 2006;8:46–54. [PubMed: 16341206]
13. Rabenstein DL. Heparin and heparan sulfate: structure and function. Nat Prod Rep 2002;19:312–331. [PubMed: 12137280]

NIH-PA Author Manuscript NIH-PA Author Manuscript NIH-PA Author Manuscript

14. Mislick KA, Baldeschwieler JD. Evidence for the role of proteoglycans in cation-mediated gene transfer. Proc Natl Acad Sci U S A 1996;93:12349–12354. [PubMed: 8901584]
15. Mounkes LC, Zhong W, Cipres-Palacin G, Heath TD, Debs RJ. Proteoglycans mediate cationic liposome-DNA complex-based gene delivery in vitro and in vivo. J Biol Chem 1998;273:26164–26170. [PubMed: 9748298]
16. Belting M. Heparan sulfate proteoglycan as a plasma membrane carrier. Trends Biochem Sci 2003;28:145–151. [PubMed: 12633994]
17. Kopatz I, Remy JS, Behr JP. A model for non-viral gene delivery: through syndecan adhesion molecules and powered by actin. J Gene Med 2004;6:769–776. [PubMed: 15241784]
18. Hacker U, Nybakken K, Perrimon N. Heparan sulphate proteoglycans: the sweet side of development. Nat Rev Mol Cell Biol 2005;6:530–541. [PubMed: 16072037]
19. Yanagishita M, Hascall VC. Cell surface heparan sulfate proteoglycans. J Biol Chem 1992;267:9451–9454. [PubMed: 1577788]
20. Hausser H, Kresse H. Decorin endocytosis: structural features of heparin and heparan sulphate oligosaccharides interfering with receptor binding and endocytosis. Biochem J 1999;344:827–835. [PubMed: 10585870]
21. Fuki IV, Meyer ME, Williams KJ. Transmembrane and cytoplasmic domains of syndecan mediate a multi-step endocytic pathway involving detergent-insoluble membrane rafts. Biochem J 2000;351:607–612. [PubMed: 11042114]
22. Fransson LA, Belting M, Cheng F, Jonsson M, Mani K, Sandgren S. Novel aspects of glypican glycobiology. Cell Mol Life Sci 2004;61:1016–1024. [PubMed: 15112050]
23. Boussif O, Lezoualc'h F, Zanta MA, Mergny MD, Scherman D, Demeneix B, Behr JP. A versatile vector for gene and oligonucleotide transfer into cells in culture and in vivo: polyethylenimine. Proc Natl Acad Sci U S A 1995;92:7297–7301. [PubMed: 7638184]
24. Thomas M, Lu JJ, Ge Q, Zhang C, Chen J, Klibanov AM. Full deacylation of polyethylenimine dramatically boosts its gene delivery efficiency and specificity to mouse lung. Proc Natl Acad Sci U S A 2005;102:5679–5684. [PubMed: 15824322]
25. Schwarze SR, Hruska KA, Dowdy SF. Protein transduction: unrestricted delivery into all cells? Trends Cell Biol 2000;10:290–295. [PubMed: 10856932]
26. Lewin M, Carlesso N, Tung CH, Tang XW, Cory D, Scadden DT, Weissleder R. Tat peptide-derivatized magnetic nanoparticles allow in vivo tracking and recovery of progenitor cells. Nat Biotechnol 2000;18:410–414. [PubMed: 10748521]
27. Fuchs SM, Raines RT. Pathway for polyarginine entry into mammalian cell. Biochemistry 2004;43:2438–2444. [PubMed: 14992581]
28. Belting M, Petersson P. Protective role for proteoglycans against cationic lipid cytotoxicity allowing optimal transfection efficiency in vitro. Biochem J 1999;342:281–286. [PubMed: 10455012]
29. Sandgren S, Cheng F, Belting M. Nuclear targeting of macromolecular polyanions by an HIV-Tat derived peptide-role for cell surface proteoglycans. J Biol chem 2002;277:38877–38883. [PubMed: 12163493]
30. Sandgren S, Wittrup A, Cheng F, Jonsson M, Eklund E, Busch S, Belting M. The human antimicrobial peptide LL-37 transfers extracellular DNA plasmid to the nuclear compartment of mammalian cells via lipid rafts and proteoglycan-dependent endocytosis. J Biol Chem 2004;279:17951–17956. [PubMed: 14963039]
31. Baeuerle PA, Huttner WB. Chlorate - a potent inhibitor of protein sulfation in intact cells. Biochem Biophys Res Commun 1986;141:870–877. [PubMed: 3026396]
32. Esko JD, Stewart TE, Taylor WH. Animal cell mutants defective in glycosaminoglycan biosynthesis. Proc Natl Acad Sci U S A 1985;82:3197–3201. [PubMed: 3858816]
33. Esko JD, Rostand KS, Weinke JL. Tumor formation dependent on proteoglycan biosynthesis. Science 1988;241:1092–1096. [PubMed: 3137658]
34. Hopkins CR. Intracellular routing of transferrin and transferrin receptors in epidermoid carcinoma A431-Cells. Cell 1983;35:321–330. [PubMed: 6313227]
35. Hopkins CR, Trowbridge IS. Internalization and processing of transferring and the transferrin receptor in human carcinoma A431-Cells. J Cell Biol 1983;97:508–521. [PubMed: 6309862]

NIH-PA Author Manuscript

NIH-PA Author Manuscript

NIH-PA Author Manuscript

36. Ma S, Chisholm RL. Cytoplasmic dynein-associated structures move bidirectionally in vivo. J Cell Sci 2002;115:1453–1460. [PubMed: 11896193]
37. Bausinger R, von Gersdorff K, Braeckmans K, Ogris M, Wagner E, Brauchle C, Zumbusch A. The transport of nanosized gene carriers unraveled by live-cell imaging. Angew Chem Int Ed 2006;45:1568–1572.
38. Norkin LC. Caveolae in the uptake and targeting of infectious agents and secreted toxins. Adv Drug Deliv Rev 2001;49:301–315. [PubMed: 11551401]
39. Pelkmans L, Burli T, Zerial M, Helenius A. Caveolin-stabilized membrane domains as multifunctional transport and sorting devices in endocytic membrane traffic. Cell 2004;118:767–780. [PubMed: 15369675]
40. Macia E, Ehrlich M, Massol R, Boucrot E, Brunner C, Kirchhausen T. Dynasore, a cell-permeable inhibitor of dynamin. Dev Cell 2006;10:839–850. [PubMed: 16740485]
41. Damke H, Baba T, Warnock DE, Schmid SL. Induction of mutant dynamin specifically blocks endocytic coated vesicle formation. J Cell Biol 1994;127:915–934. [PubMed: 7962076]
42. Chavrier P, Parton RG, Hauri HP, Simons K, Zerial M. Localization of low molecular weight GTP binding proteins to exocytic and endocytic compartments. Cell 1990;62:317–329. [PubMed: 2115402]
43. Sonnichsen B, De Renzis S, Nielsen E, Rietdorf J, Zerial M. Distinct membrane domains on endosomes in the recycling pathway visualized by multicolor imaging of Rab4, Rab5, and Rab11. J Cell Biol 2000;149:901–914. [PubMed: 10811830]
44. Barbero P, Bittova L, Pfeffer SR. Visualization of Rab9-mediated vesicle transport from endosomes to the trans-Golgi in living cells. J Cell Biol 2002;156:511–518. [PubMed: 11827983]
45. Rink J, Ghigo E, Kalaidzidis Y, Zerial M. Rab conversion as a mechanism of progression from early to late endosomes. Cell 2005;122:735–749. [PubMed: 16143105]
46. Vonderheit A, Helenius A. Rab7 associates with early endosomes to mediate sorting and transport of Semliki forest virus to late endosomes. PLoS Biol 2005;3:e233. [PubMed: 15954801]
47. Lakadamyali M, Rust MJ, Zhuang X. Ligands for clathrin-mediated endocytosis are differentially sorted into distinct populations of early endosomes. Cell 2006;124:997–1009. [PubMed: 16530046]
48. Goldstein JL, Brown MS, Anderson RG, Russell DW, Schneider WJ. Receptor-mediated endocytosis: concepts emerging from the LDL receptor system. Annu Rev Cell Biol 1985;1:1–39. [PubMed: 2881559]
49. Dunn KW, McGraw TE, Maxfield FR. Iterative fractionation of recycling receptors from lysosomally destined ligands in an early sorting endosome. J Cell Biol 1989;109:3303–3314. [PubMed: 2600137]
50. Apodaca G. Endocytic traffic in polarized epithelial cells: role of the actin and microtubule cytoskeleton. Traffic 2001;2:149–159. [PubMed: 11260520]
51. Li G, D'Souza-Schorey C, Barbieri MA, Roberts RL, Klippel A, Williams LT, Stahl PD. Evidence for phosphatidylinositol 3-kinase as a regulator of endocytosis via activation of Rab5. Proc Natl Acad Sci U S A 1995;92:10207–10211. [PubMed: 7479754]
52. Simonsen A, Lippe R, Christoforidis S, Gaullier JM, Brech A, Callaghan J, Toh BH, Murphy C, Zerial M, Stenmark H. EEA1 links PI(3)K function to Rab5 regulation of endosome fusion. Nature 1998;394:494–498. [PubMed: 9697774]
53. Petiot A, Faure J, Stenmark H, Gruenberg J. PI3P signaling regulates receptor sorting but not transport in the endosomal pathway. J Cell Biol 2003;162:971–979. [PubMed: 12975344]
54. Gruenberg J, Stenmark H. The biogenesis of multivesicular endosomes. Nat Rev Mol Cell Biol 2004;5:317–323. [PubMed: 15071556]
55. Martys JL, Wjasow C, Gangi DM, Kielian MC, McGraw TE, Backer JM. Wortmannin-sensitive trafficking pathways in Chinese hamster ovary cells. Differential effects on endocytosis and lysosomal sorting. J Biol Chem 1996;271:10953–10962. [PubMed: 8631914]
56. Shpetner H, Joly M, Hartley D, Corvera S. Potential sites of PI-3 kinase function in the endocytic pathway revealed by the PI-3 kinase inhibitor, wortmannin. J Cell Biol 1996;132:595–605. [PubMed: 8647891]
57. Mellman I. Endocytosis and molecular sorting. Annu Rev Cell Dev Biol 1996;12:575–625. [PubMed: 8970738]

NIH-PA Author Manuscript

NIH-PA Author Manuscript

NIH-PA Author Manuscript

58. Nichols BJ, Kenworthy AK, Polishchuk RS, Lodge R, Roberts TH, Hirschberg K, Phair RD, Lippincott-Schwartz J. Rapid cycling of lipid raft markers between the cell surface and Golgi complex. J Cell Biol 2001;153:529–541. [PubMed: 11331304]

59. Motley A, Bright NA, Seaman MNJ, Robinson MS. Clathrin-mediated endocytosis in AP-2-depleted cells. J Cell Biol 2003;162:909–918. [PubMed: 12952941]

NIH-PA Author Manuscript

NIH-PA Author Manuscript

NIH-PA Author Manuscript

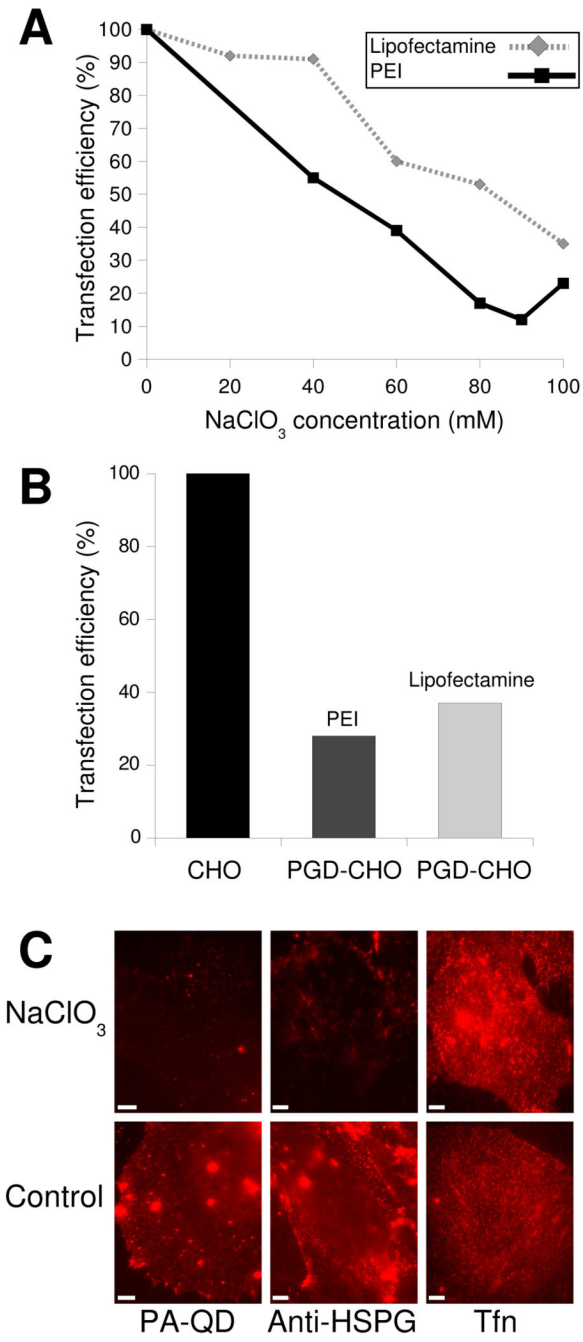

Figure 1. Cellular entry of cationic polymers, lipids, and polypeptides is mediated by cell surface proteoglycans

A) Transfection of BS-C-1 cells by PEI and LF is inhibited by sodium chlorate, a drug that inhibits proteoglycan synthesis, in a concentration dependent manner. B) Transfection by PEI and LF is much less efficient in a proteoglycan-deficient cell line of CHO cells (PGD-CHO) than in wildtype CHO cells. Transfection efficiencies are normalized against untreated cells. Based on experiments done in triplicate, the error in the transfection measurement is 10%. C) Sodium chlorate ($NaClO_3$, 80 mM) treatment blocks the binding of PA-QDs and anti-HSPG, but not that of transferrin (Tfn), to the surface of BS-C-1 cells. The diffuse red signal in the

images is due to out of focus fluorescence on the thicker regions of the cells. Scale bars: 10 μm.

NIH-PA Author Manuscript

NIH-PA Author Manuscript

NIH-PA Author Manuscript

NIH-PA Author Manuscript
NIH-PA Author Manuscript
NIH-PA Author Manuscript

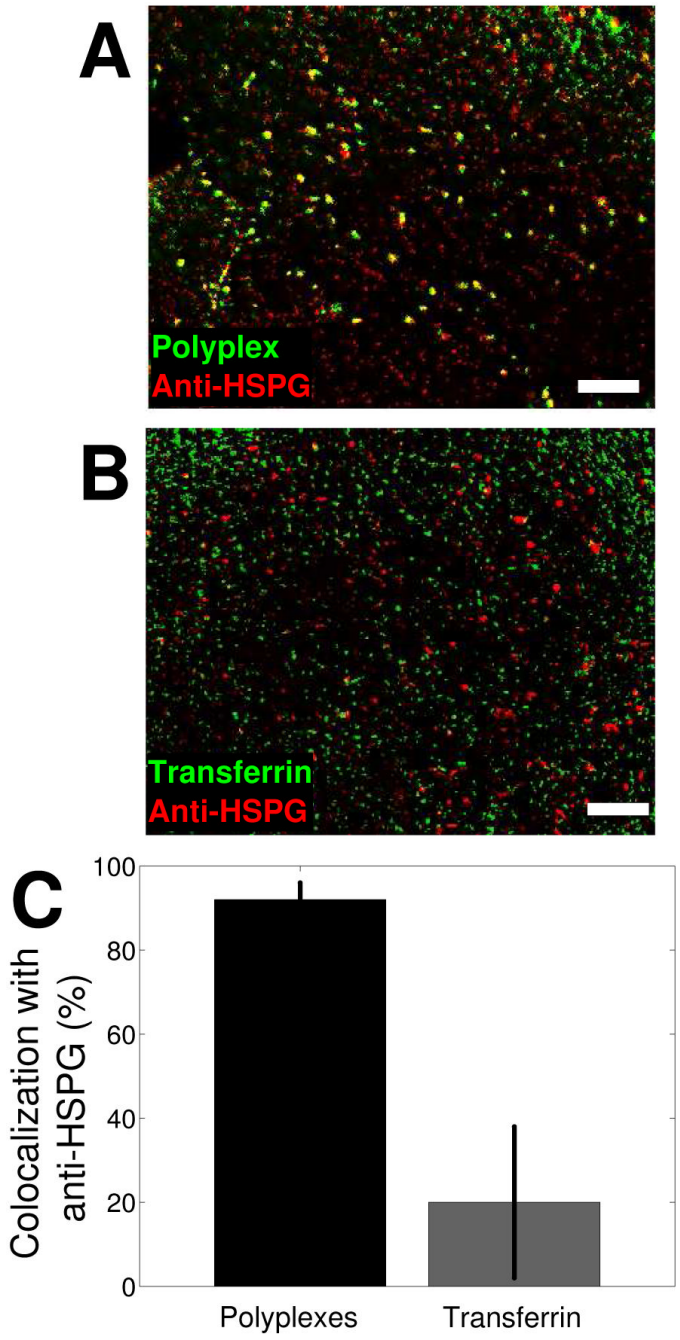

Figure 2. Polyplexes colocalize with a heparan sulfate antibody (anti-HSPG)

A) Polyplex (green) and anti-HSPG (red) after 20 minutes incubation with cells. Colocalization is shown in yellow. B) Tranferrin (green) and anti-HSPG (red) after 20 minutes incubation with cells. Scale bars: 10 μm. C) Percent colocalization of polyplexes and transferrin with anti-HSPG averaged from 5 to 30 minutes following binding.

NIH-PA Author Manuscript
NIH-PA Author Manuscript
NIH-PA Author Manuscript

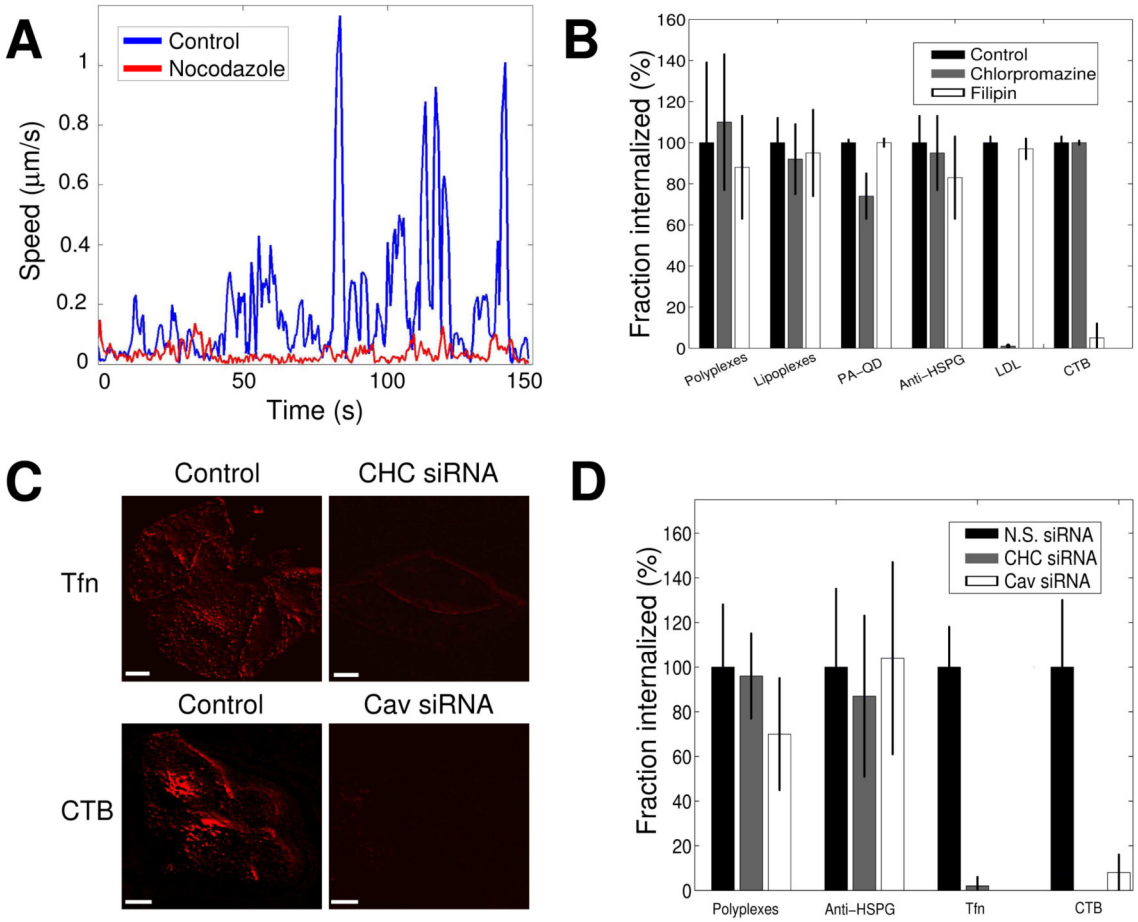

Figure 3. Endocytosis of polyplexes, lipoplexes, PA-QDs, and anti-HSPG is independent of clathrin or caveolin

A) Microtubule-dependent motion (blue) of a vesicle containing polyplexes inside a cell. About 95% of vesicles containing polyplexes exhibit this type of movement. This rapid movement is inhibited when microtubules are disrupted with nocodazole (red). B) Amount of polyplexes, lipoplexes, PA-QDs, anti-HSPG, low-density lipoprotein (LDL), and cholera toxin B (CTB) that entered cells within 30 minutes for untreated cells (control) and cells treated with chlorpromazine or filipin. All results are normalized against untreated cells. C) Representative images of control cells transfected with non-specific siRNA, cells transfected with siRNA against clathrin heavy chain (CHC), and cells transfected with siRNA against caveolin-1 (Cav) 30 minutes following the addition of Alexa647-labeled transferrin (Tfn) or CTB. Transferrin or CTB that remained on the cell surface was removed with an acid wash. Scale bars: 10 μm. D) Fraction of polyplexes, anti-HSPG, transferrin (Tfn), and CTB that have entered cells within 30 minutes in control cells transfected with non-specific siRNA and clathrin or caveolin-1 knockdown cells.

NIH-PA Author Manuscript

NIH-PA Author Manuscript

NIH-PA Author Manuscript

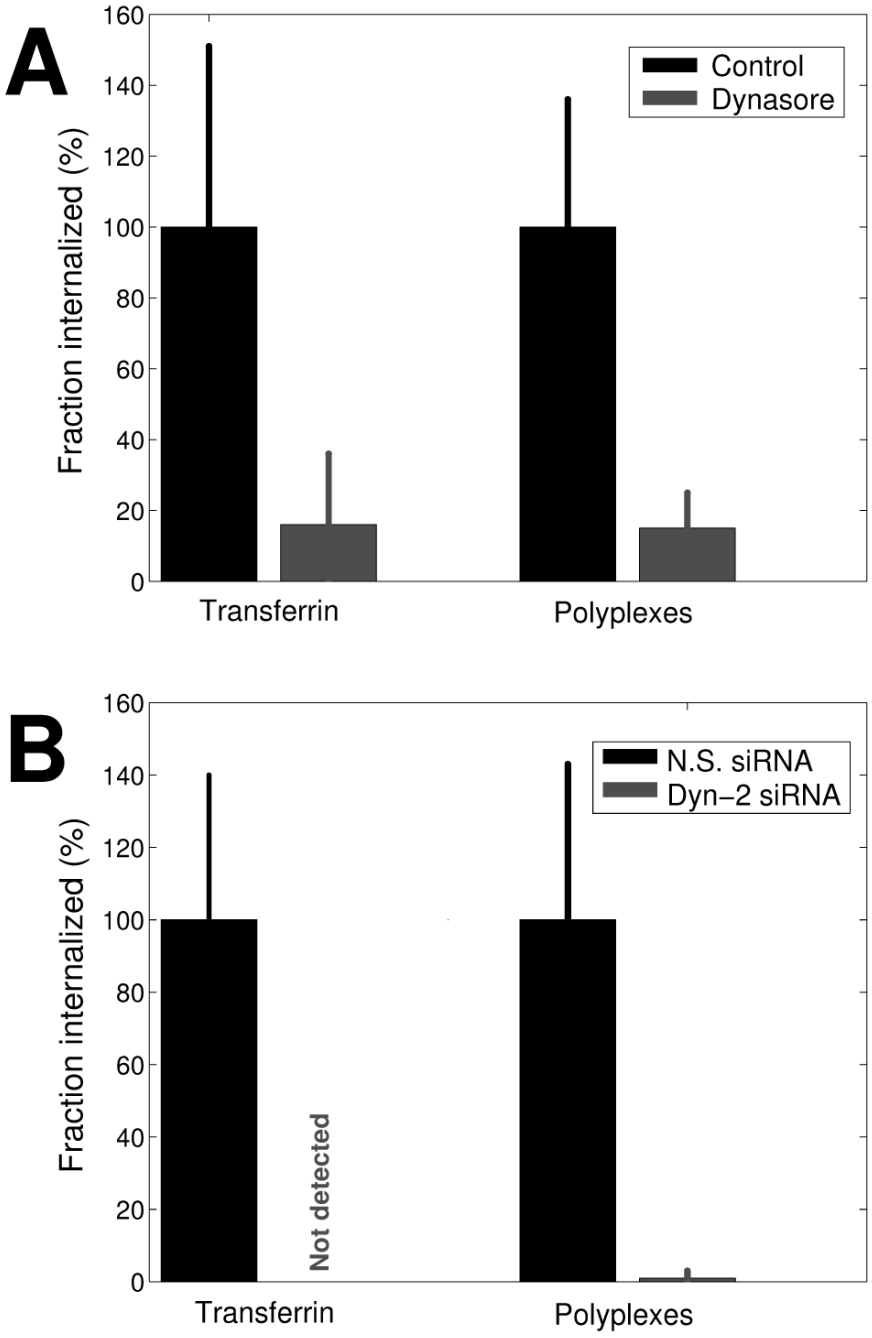

Figure 4. Internalization of polyplexes requires dynamin-2

A) Fraction of transferrin and polyplexes that have entered cells within 30 minutes in control cells and Dynasore-treated cells. B) Fraction of transferrin and polyplexes that have entered cells within 30 minutes in control cells transfected with non-specific siRNA and in cells transfected with siRNA against dynamin-2.

NIH-PA Author Manuscript
NIH-PA Author Manuscript
NIH-PA Author Manuscript

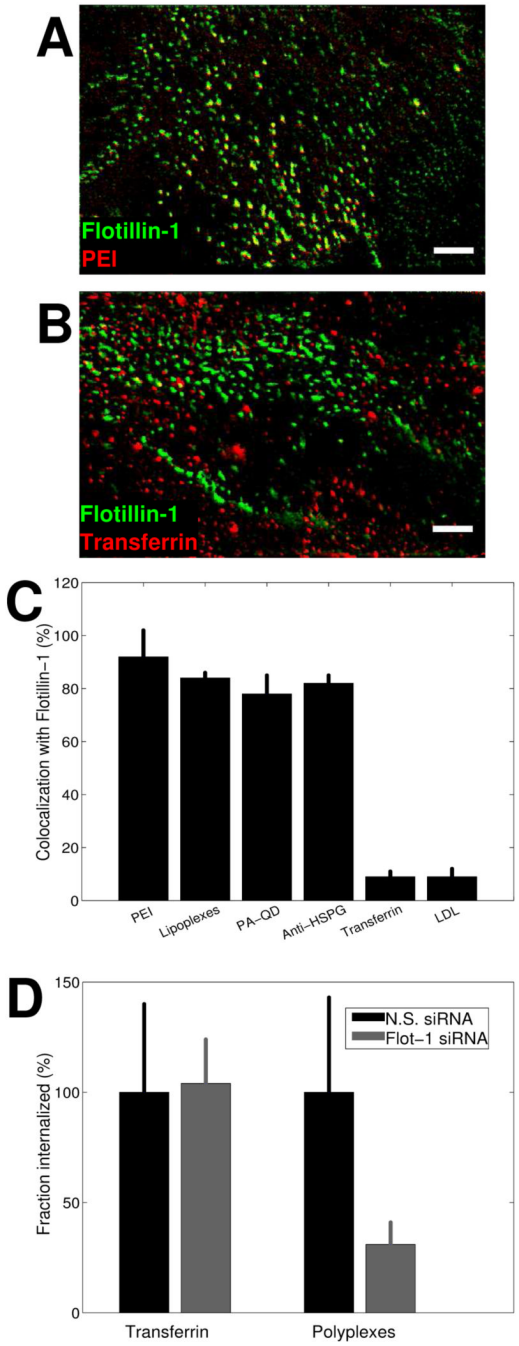

Figure 5. Cationic ligands and anti-HSPG colocalize with flotillin-1 at early times post-endocytosis

A) PEI (red) and EGFP-flotillin-1 (green) at 10 minutes post-endocytosis. Colocalization is shown in yellow. B) Transferrin (red) and EGFP-flotillin-1 (green) at 10 minutes post-endocytosis. Scale bars: 10 μm. C) PEI, lipoplexes, PA-QDs, and anti-HSPG all show extensive colocalization with flotillin-1 vesicles within the first 20 minutes of entry. In comparison, transferrin and LDL, both clathrin-dependent ligands show less than 10% colocalization with flotillin-1. D) Fraction of transferrin and polyplexes that have entered cells within 30 minutes in control cells transfected with non-specific siRNA and in cells transfected with siRNA against flotillin-1.

NIH-PA Author Manuscript
NIH-PA Author Manuscript
NIH-PA Author Manuscript

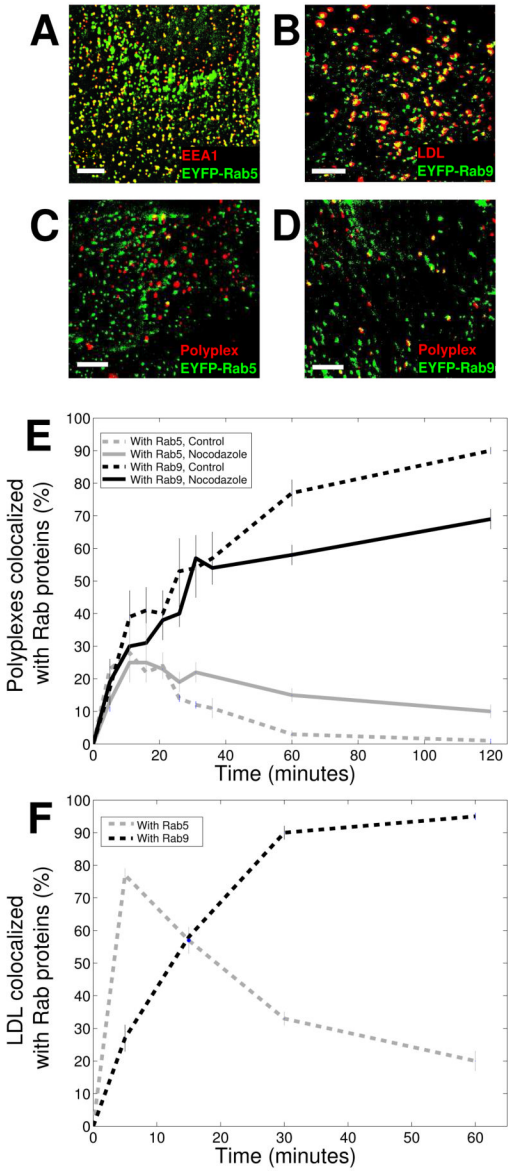

Figure 6. Proteoglycans and proteoglycan-binding ligands are trafficked to late endosomes with high efficiency

A) Colocalization between EYFP-Rab5 (green) and EEA1 (red), an early endosomal marker. EEA1 was detected by immunofluorescence. Image adapted from Lakadamyali, *et al*. (43). B) Colocalization between EYFP-Rab9 (green) and DiD-labeled LDL (red). The image was taken 1 hour after LDL internalization, at which point LDL accumulates in late endosomes. C) A two-color image of polyplexes and EYFP-Rab5, an early endosomal marker, 20 minutes after the addition of polyplexes to cells. D) A two-color image of polyplexes and EYFP-Rab9, a late endosomal marker, 1 hour after the addition of polyplexes to cells. Colocalization is shown in yellow. Scale bars: 10 μm. E) Fraction of polyplexes colocalized with Rab5 (gray) and Rab9 (black) as a function of time. The solid and dashed lines indicate results from cells treated with nocodazole and untreated cells, respectively. . Error bars indicate standard error. Results were averaged over 5 cells. F) Fraction of LDL particles colocalized with Rab5 (gray) and Rab9 (black) as a function of time in untreated cells. Error bars indicate standard error. Results were averaged over 4 - 7 cells.

NIH-PA Author Manuscript
NIH-PA Author Manuscript
NIH-PA Author Manuscript

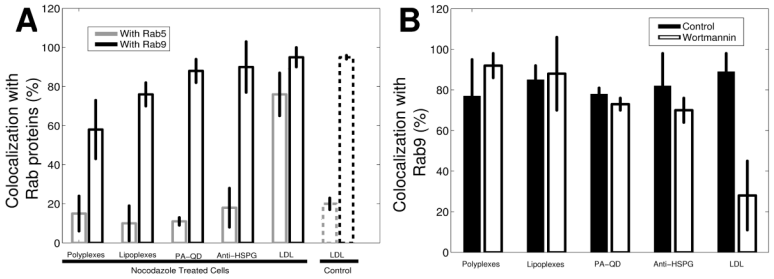

Figure 7. Proteoglycans and proteoglycan-binding ligands are trafficked to late endosomes independently of microtubule-dependent motion or PI(3)K-dependent sorting from early endosomes

A) Fraction of polyplexes, lipoplexes, PA-QDs, anti-HSPG, and LDL colocalized with Rab5 (gray) and Rab9 (black) at 1 hour after incubation with nocodazole-treated cells (solid columns). The majority of polyplexes, lipoplexes, PA-QDs, and anti-HSPG accumulate in endosomes that contain only Rab 9 but not Rab5. In contrast, the majority of LDL particles colocalize with both Rab5 and Rab9. The dashed columns show results for LDL in untreated control cells for comparison. Error bars indicate standard deviation. G) PtdIns3P-dependent sorting from early endosomes is not required for late endosomal entry of cationic ligands and HSPG. Fraction of polyplexes, lipoplexes, PA-QDs, and anti-HSPG in late endosomes that contain Rab9, but not Rab5, is similar in untreated cells and in cells treated with wortmannin, an inhibitor of PI(3)K. In comparison, colocalization of LDL with Rab9 is substantially reduced by wortmannin treatment. Measurements were done 1 hour post-endocytosis. Error bars indicate standard deviation.